Research Square

Preprints are preliminary reports that have not undergone peer review.
They should not be considered conclusive, used to inform clinical practice,
or referenced by the media as validated information.

Monomeric ASC inhibits α-synuclein aggregation through its CARD domain

Kohta Hirayama
The University of Tokyo
Hiroto Kobayashi
The University of Tokyo
Ikumi Tomizawa
The University of Tokyo
Yukiko Hori
The University of Tokyo
Taisuke Tomita
taisuke@mol.f.u-tokyo.ac.jp

The University of Tokyo

Article

Keywords:

Posted Date: November 9th, 2026

DOI: https://doi.org/10.21203/rs.3.rs-11369461/v1

License: This work is licensed under a Creative Commons Attribution 4.0 International License.
Read Full License

Additional Declarations: No competing interests reported.

Monomeric ASC inhibits α-synuclein aggregation through its CARD domain

Kohta Hirayama[1#], Hiroto Kobayashi[1#], Ikumi Tomizawa[1#], Yukiko Hori[1], Taisuke Tomita[1]

[1] Laboratory of Neuropathology and Neuroscience, Graduate School of Pharmaceutical Sciences, The University of Tokyo

[#]These authors contributed equally to this work.

*Correspondence: Y.H., yukiko-hori@mol.f.u-tokyo.ac.jp

*Correspondence: T.T., taisuke@mol.f.u-tokyo.ac.jp

Abstract

Synucleinopathies, including Parkinson disease, are characterized by the pathological aggregation of α-synuclein (α-syn) in the brain, which promotes neurodegeneration and inflammation. While inflammasome activation is implicated in disease progression, the direct role of the inflammasome adaptor protein ASC in α-syn aggregation remains unclear. Here we demonstrate that ASC monomers directly bind α-syn fibrils via their CARD domain, inhibiting α-syn aggregation both *in vitro* and in cultured cells. This interaction reduces seeded α-syn fibrillization without altering fibril structure, suggesting a protective mechanism by steric hindrance. Moreover, ASC overexpression decreases intracellular α-syn aggregation, indicating functional relevance in cells. These findings suggest that maintaining monomeric ASC, potentially through inflammasome inhibition, may mitigate α-syn pathology and associated neurodegeneration. Thus, targeting ASC dynamics offers a promising avenue for therapeutic intervention in synucleinopathies.

Introduction

Synucleinopathies are a group of neurodegenerative diseases caused by the abnormal accumulation of aggregated, fibrillar α-synuclein (α-syn) in neurons and glial cells[1–6]. Major synucleinopathies include Parkinson disease (PD), dementia with Lewy bodies (DLB), and multiple system atrophy (MSA). In PD and DLB, α-syn accumulates as Lewy bodies and Lewy neurites in neuronal cells, while α-syn accumulates as glial cytoplasmic inclusions in MSA[7]. This accumulated α-syn is known to create amyloid filaments with a cross-β-sheet structure, acquiring insolubility to detergents such as sarkosyl[8,9]. Aggregated α-syn propagates between cells in a prion-like manner, seeding further aggregation in the propagated cells[10–13]. The aggregation of α-syn is associated with cellular toxicity, which contributes to neurodegeneration and provokes inflammatory responses in the brains of affected individuals. Therefore, targeting the inhibition of α-syn aggregation and its propagation represents a promising therapeutic strategy to slow or prevent the progression of synucleinopathies.

In disease brains, aggregated α-syn evokes inflammatory responses. One of the responses activated by α-syn is the formation of NLRP3 inflammasomes[14], protein complexes that mediate the secretion of interleukin-1β (IL-1β). The NLRP3 inflammasome is composed of NLRP3, ASC, and caspase-1, and the homotypic

intermolecular interactions between the pyrin domains (PYD) of NLRP3 and ASC, and the caspase recruitment domains (CARD) of ASC and caspase-1 lead to the autoproteolytic cleavage and activation of caspase-1[15]. Activated caspase 1 cleaves pro-IL-1β to IL-1β, leading to its release and triggering inflammatory responses in surrounding cells as well[16]. Recent studies have shown that NLRP3 knockout and inflammasome inhibitors can improve α-syn pathology in PD model mice[17–19], suggesting the significance of inflammasome formation in the pathogenesis of synucleinopathies.

The adaptor protein ASC is a common adaptor between inflammasomes, and can also polymerize into ASC specks[20,21]. The formation of ASC specks can also be triggered by α-syn aggregation, and can trigger inflammatory responses as well. Moreover, increased expression of ASC has been reported in PD patients[18], suggesting the involvement of ASC in the pathological process of synucleinopathies. Beyond its role in inflammation, ASC specks have been reported to cross-seed amyloid-β, an amyloid protein known to be aggregated in Alzheimer disease, another neurodegenerative disease caused by protein aggregation[22,23].

Although accumulating evidence links α-syn pathology to inflammasome activation, the direct molecular relationship between ASC and α-syn has not been fully elucidated. In this study, we investigated the interaction between ASC and α-syn proteins

and found that ASC binds specifically to α-syn fibrils, inhibiting their aggregation both in vitro and in cultured cells. This interaction is mediated by the CARD domain of ASC. Furthermore, overexpression of ASC in cells promoted its association with transfected α-syn fibrils and resulted in reduced α-syn aggregation. Our findings suggest that monomeric ASC plays a protective role by inhibiting α-syn aggregation, whereas the assembly of ASC into specks or its incorporation into inflammasomes may interfere with this inhibitory interaction.

Materials and methods

Antibodies

The following antibodies were purchased and used in the experiments: mouse anti-α-syn antibody 4D6 (834303, BioLegend, CA, USA, 1:1000 dilution), mouse anti-α-syn antibody Clone 42 (610786, Becton, Dickinson and Company, NJ, USA, 1:1000 dilution), rabbit anti-phosphorylated α-syn antibody EP1536Y (ab51253, Abcam, Cambridge, UK, 1:1000 dilution), rabbit anti-ASC antibody D2W8U (#67824, Cell Signaling Technology, MA, USA, 1:1000 dilution), rabbit anti-ASC antibody A1170 (A1170, ABclonal, Hubei, China, 1:1000 dilution), rabbit anti-ASC antibody AL177 (AG-25B-0006-C100, AdipoGen, CA, USA, 1:1000 dilution), mouse anti-FLAG antibody M2 (F3165, Merck, Darmstadt, Germany, 1:1000 dilution), mouse anti-FLAG antibody 1E6 (014-22383, FUJIFILM Wako Pure Chemical Corporation, Osaka, Japan, 1:1000 dilution), mouse anti-α-tubulin antibody DM1A (T9026, Merck, Darmstadt, Germany, 1:1000 dilution), horseradish peroxidase-conjugated sheep anti-mouse IgG antibody (#515-035-003, Jackson ImmunoResearch, PA, USA), horseradish peroxidase-conjugated goat anti-rabbit IgG antibody (#111-035-003, Jackson ImmunoResearch, PA, USA), Alexa Fluor 488 AffiniPure donkey anti-mouse IgG antibody (#715-545-151, Jackson ImmunoResearch, PA, USA), Cy3 AffiniPure Donkey Anti-Rabbit IgG (#711-

165-152, Jackson ImmunoResearch, PA, USA).

Preparation of recombinant α-syn

The recombinant human wild-type (WT) α-syn (cloned into pRK127 vector) plasmid was a kind gift from Dr. Masato Hasegawa at the Tokyo Metropolitan Institute of Medical Science[24].

Recombinant α-syn was purified according to previous reports [24–27]. Briefly, the WT α-syn was expressed in BL21 (DE3) (Nippon gene CO., LTD., Tokyo, Japan), and were purified using an anion exchange chromatography column. The eluted α-syn was precipitated with ammonium sulfate dissolved in 30 mM Tris-HCl (pH 7.5) (2-Amino-2-(hydroxymethyl)-propane-1,3-diol [Tris] (FUJIFILM Wako Pure Chemical Corporation, Osaka, Japan), Hydrochloric Acid (FUJIFILM Wako Pure Chemical Corporation, Osaka, Japan)). Ions were then removed by dialysis and aggregates were removed by ultracentrifugation. Protein concentrations were measured using a BCA protein assay kit (Takara Bio, Shiga, Japan) according to the manufacturer's instructions. Resultant α-syn monomers were stored at -80°C until use.

Recombinant α-syn seed preparation

For fibrillization, 5 mg/mL monomeric recombinant α-syn was shaken at 1,000 rpm, 37°C for 5 days[27,28]. To remove monomers, the fibrillar α-syn was ultracentrifuged at 45,000 rpm, 25°C for 20 minutes. The resulting pellet was solubilized as seeds by sonication, and the concentration was measured by BCA assay. The seeds were stored at -80°C until use.

Recombinant ASC purification

The pET-15b vector with His tag was a kind gift from Dr. Kiyotaka Tokuraku of Muroran Institute of Technology. FLAG-ASC sequence was cloned from pcDNA3-N-Flag-ASC1 (Addgene #75134) on to this vector using NEBuilder HiFi DNA Assembly (New England Biolab, MA, USA). The PYD and CARD domains were amplified and assembled using respective primers indicated below.

PYD forward: CTCTTCTTTAGTCGTTTGCAGCTGCTC

PYD reverse: TGCAAACGACTAAAGAAGAGTGAGGATCCGGCTGCTAACAAAGC

CARD forward: GCTCAGAGTACAGCCAGAACAGG

CARD reverse: CTGGCTGTACTCTGAGCTTTATCGTCATCGTCTTTGTAGTCCTCGAG

ASC, PYD, and CARD were expressed in Rosetta2 (DE3) pLysS competent cells (Merck, Darmstadt, Germany) and purified using Ni-NTA agarose beads (FUJIFILM Wako Pure Chemical Corporation, Osaka, Japan) according to the manufacturer's instructions with minor modifications. Cells were sonicated in 50 mM HEPES-NaOH (FUJIFILM Wako Pure Chemical Corporation, Osaka, Japan) (pH 8.0), 250 mM NaCl (FUJIFILM Wako Pure Chemical Corporation, Osaka, Japan), 0.2% (v/v) Triton X-100 (FUJIFILM Wako Pure Chemical Corporation, Osaka, Japan), 1 mM DTT (Nacalai Tesque, Kyoto, Japan), Complete EDTA-free (Roche), 10 mg/mL lysozyme (FUJIFILM Wako Pure Chemical Corporation, Osaka, Japan), 3,000 units/L culture benzonase (Merck, Darmstadt, Germany). The lysates were centrifuged at 12,000 g, 4°C, 30 minutes. A final concentration of 10% (v/v) glycerol (FUJIFILM Wako Pure Chemical Corporation, Osaka, Japan), 50 μM ATP (Merck, Darmstadt, Germany), 20 mM imidazole (FUJIFILM Wako Pure Chemical Corporation, Osaka, Japan) were added to the supernatant, and filtered with 0.45 μm PES filter (Merck, Darmstadt, Germany). 0.5 mL of Ni-NTA agarose beads washed three times with 50 mM HEPES-NaOH (pH 8.0), 250 mM NaCl were added to the samples and rotated at 4°C for 1 hour. The samples were loaded onto 10 mL Chromatography Columns (Bio-Rad, CA, USA) and washed with 5 mL of wash

buffer (50 mM HEPES-NaOH (pH 8.0), 250 mM NaCl, 0.2% (v/v) Triton-X 100, 0.03% (w/v) Brij-35 (Kanto Chemical), 50 μM ATP, 1 mM DTT, 20 mM imidazole). Proteins were eluted 6 times with 0.5 mL of wash buffer with imidazole at a final concentration of 500 mM. Eluted proteins were dialyzed in 30 mM Tris-HCl (pH 7.5). Aggregates were removed by ultracentrifuge at 50,000 rpm, 20 minutes, 25°C. Supernatants were collected and protein concentrations were measured using BCA protein assay. The proteins were stored at -80°C until use.

Real time quaking-induced conversion (RT-QuIC)

190 μL of reaction mixtures (30 mM Tris-HCl (pH 7.5), 10 μM Thioflavin-T (Th-T; Merck, Darmstadt, Germany), 1 mg/mL α-syn monomers) with or without 1 μM ASC, PYD, or CARD were added to black bottom 96 well plates. 10 μL of 0.1 mg/mL α-syn seeds were added to each well to induce aggregation. As a positive control to calculate lag time, 10 μL of 0.4 mg/mL α-syn seeds were added. 10 μL of 30 mM Tris-HCl (pH7.5) were added as negative controls. Plates were incubated in a microplate reader (TECAN) at 37°C, 1 minute of shaking for each kinetic cycle of 30 minutes for a total of 168 hours. Th-T fluorescence was measured at an integration time of 20 μs. Each sample was measured in six replicate wells, and the number of independent experiments (n) is

indicated in each figure legend. Samples were collected and ultracentrifuged at 50,000 rpm, 25°C for 20 minutes and the supernatant and pellet were collected for immunoblotting.

Immunoprecipitation

50 μL of Protein G magnetic beads (Thermo Fisher Scientific) were washed 3 times with 175 μL of wash buffer (30 mM Tris-HCl (pH 7.5), 0.05% Tween-20 (Merck, Darmstadt, Germany)) and once with MilliQ. 1-10 μg of antibodies were added to the magnetic beads and rotated for 30 minutes at room temperature. The beads were washed 3 times using wash buffer. 500 μL of samples with 5 μM of recombinant ASC peptides and 5 μM of α-syn monomers in 30 mM Tris-HCl (pH 7.5) pre-incubated for 1 hour at 37 °C, 1,000 rpm (input samples) were added to the magnetic beads. After 1 hour of rotation at room temperature, the supernatant was collected as the unbound samples. The beads were washed 3 times with wash buffer and once with MilliQ, and the final beads were resuspended in 1 x sample buffer (2% SDS, 80 mM Tris-HCl (pH6.8), 15% glycerol, 0.0025% Brilliant green (FUJIFILM Wako Pure Chemical Corporation, Osaka, Japan), 0.00625% Coomassie Brilliant Blue G-250 (Nacalai Tesque, Kyoto, Japan)) as the pulldown sample.

Co-precipitation of ASC and α-syn

100 μL of 10 μM α-syn seeds or monomers and 1 μM of ASC, PYD, and CARD monomers in 30 mM Tris-HCl (pH 7.5) were incubated at 1,000 rpm, 37°C for 1 hour. The samples were ultracentrifuged at 50,000 rpm, 25°C for 30 minutes, and the supernatants were collected. The pellets were washed with 500 μL of 30 mM Tris-HCl (pH 7.5) and resuspended in 100 μL 30 mM Tris-HCl (pH 7.5) by sonication.

Cell culture and seeded aggregation of α-syn

SH-SY5Y cells were a gift from Dr. Masato Hasegawa. SH-SY5Y cells were cultured in Dulbecco's Modified Eagle Medium/Nutrient Mixture F-12 (Thermo Fisher Scientific, MA, USA) supplemented with 1% Minimum Essential Medium Non-Essential Amino Acids (Thermo Fisher Scientific, MA, USA), 10% fetal bovine serum (Cosmo Bio, Tokyo, Japan) and 50 units/mL penicillin and streptomycin (Thermo Fisher Scientific, MA, USA), and maintained at 37°C in a 5% CO_2, 95% air atmosphere incubator[27,29].

Monoclonal SH-SY5Y cells stably expressing α-syn were generated using lentiviral infection as previously described[27,29]. Overexpression of ASC was conducted using Polyethyleneimine Max (Polysciences, PA, USA) according to the manufacturer’s

instructions. Monoclonal SH-SY5Y cells stably expressing α-syn and ASC were generated by transfection of ASC plasmids to α-syn stable SH-SY5Y cells followed by antibiotic selection.

α-syn seeds with or without ASC were transfected using MultiFectam (Promega, WI, USA) as previously described[27,30]

Immunocytochemistry

For immunocytochemistry, cells were plated onto 12 well plates with 12 mm glass coverslips. Cells were fixed with 4% paraformaldehyde in PBS (FUJIFILM Wako Pure Chemical Corporation, Osaka, Japan) for 15 minutes at room temperature and washed with PBS. Permeabilization and blocking with 3% bovine serum albumin (BSA) (Merck, Darmstadt, Germany), 0.1% Triton X-100 (FUJIFILM Wako Pure Chemical Corporation, Osaka, Japan) in PBS was conducted at room temperature for 30 minutes. The cells were incubated with primary antibody solution in 3% BSA, 0.1% Triton X-100 (FUJIFILM Wako Pure Chemical Corporation, Osaka, Japan) in PBS for 90 minutes at room temperature. Cells were washed with PBS 3 times, and the coverslips were mounted on slide glass using ProLong Diamond Antifade Mountant with DAPI (Thermo Fisher Scientific, MA, USA). Samples were observed using SP5 microscope (Wetzlar, Germany).

Biological analysis of sarkosyl-insoluble α-syn

Sarkosyl fractionation was conducted as previously described[27]. In brief, cells were extracted with A68 buffer (10 mM Tris-HCl (pH 7.5), 0.8 M NaCl, 1 mM EDTA, 10% sucrose(FUJIFILM Wako Pure Chemical Corporation, Osaka, Japan)) with 1% N-lauryl sarcosine (sarkosyl; Merck, Darmstadt, Germany). The extract was sonicated for 30 sec and incubated at 37°C for 30 minutes. Part of the samples were collected as the total lysate. After the ultracentrifugation at 50,000 rpm for 20 minutes at 25°C, the supernatants were collected as the sarkosyl-soluble fraction. The resulting pellets were washed with 30 mM Tris-HCl (pH 7.5) and resuspended in 30 mM Tris-HCl (pH 7.5) by 30 sec of sonication as the sarkosyl-insoluble fraction. The samples were mixed with 2 x sample buffer (4% SDS, 160 mM Tris-HCl (pH6.8), 30% glycerol, 0.005% Brilliant green (FUJIFILM Wako Pure Chemical Corporation, Osaka, Japan), 0.0125% Coomassie Brilliant Blue G-250 (Nacalai Tesque, Kyoto, Japan)) with 2% 2-mercaptoethanol (FUJIFILM Wako Pure Chemical Corporation, Osaka, Japan) and boiled for 10 minutes. Samples were stored at -30°C until use.

Proteinase K analysis

Co-precipitated α-syn and ASC, PYD, or CARD were used for analysis. 1 mg/mL proteinase K (Merck, Darmstadt, Germany) were dissolved in 30 mM Tris-HCl (pH 7.5) and kept at -30°C until use. 10 ng/μL of α-syn seeds were digested by proteinase K at a final concentration of 0.1 ng/μL for 0, 5, 15, 30, and 60 minutes at 37°C. Reactions were stopped by the addition of 2 x sample buffer with 2% mercaptoethanol and boiled at 100°C for 10 minutes.

Immunoblotting

Dot blot was performed by dropping 2 μL of each sample onto nitrocellulose membranes (GE Healthcare, IL, USA).

All procedures of western blotting were performed as previously described[29,31–33]. Protein concentrations in cell lysates were measured using BCA protein assay according to the manufacturer's instructions. Samples and protein marker, Precision Plus Protein Dual Xtra Standards (Bio-Rad, CA, USA), were applied to 7.5% Tris/Glycine or 15% Tris/Tricine SDS-PAGE gels and transferred onto PVDF membranes (Merck, Darmstadt, Germany).

Membranes with proteins were blocked with 5% (w/v) skim milk (Becton,

Dickinson and Company, NJ, USA) in TS-Tween (0.1 % Tween-20 (Merck, Darmstadt, Germany,), 50 mM Tris-HCl (pH7.6), 150 mM NaCl) for 30 minutes at room temperature. The membranes were incubated with primary antibody solutions in TS-Tween at 4°C overnight. Membranes were washed with TS-Tween and incubated with secondary antibodies for 1 hour at room temperature. Immunodetection was performed using the ImmunoStar detection kit (FUJIFILM Wako Pure Chemical Corporation, Osaka, Japan) and Image Quant LAS4000 (GE Healthcare, IL, USA).

Statistical analysis

Data analyses were conducted from independent tubes or wells and were not conducted in a blinded fashion. Data are presented as mean values and error bars indicate the standard error of the mean (SEM). Suitable statistical analysis was performed, including Tukey's HSD test, the paired-sample *t*-test, and the unpaired Student's *t*-test. A *p*-value of less than 0.05 was considered to have a statistically significant difference between groups.

Results

ASC interacts with α-syn fibrils but not monomers

To determine the interaction between α-syn and ASC, we purified recombinant ASC protein (Fig. 1A) and mixed them with α-syn monomers and fibrils. Immunoprecipitation using anti-ASC antibodies revealed that α-syn monomers do not bind to ASC (Fig. 1B, C). However, ASC monomers mixed with α-syn fibrils, but not monomers, were co-precipitated by ultracentrifugation (Fig. 1D, E), suggesting the direct interaction of ASC protein with α-syn fibrils. In the immunoprecipitation assay, neither α-syn nor ASC was recovered above the level of the control immunoglobulin G, confirming that ASC does not form a stable complex with monomeric α-syn. In the co-sedimentation assay, by contrast, ASC partitioned into the insoluble pellet only when α-syn fibrils were present and otherwise remained in the supernatant, and quantification of pelleted ASC normalized to total ASC confirmed that this fibril-dependent recruitment was reproducible across independent experiments.

ASC binding inhibits α-syn aggregation

In order to elucidate the role of ASC-α-syn interactions in synucleinopathy pathogenesis, we conducted real time quaking-induced conversion (RT-QuIC) assay. The

lag time for seeded aggregation was analyzed using the Th-T fluorescence of high concentration α-syn seeds at the beginning of each assay (Fig. 2A). Surprisingly, α-syn aggregation was delayed by ASC monomers in a dose-dependent manner, suggesting the inhibitory effect of ASC-α-syn aggregation in α-syn aggregation (Fig. 2B, C). Since the decreased Th-T fluorescence may be due to the interference of Th-T-α-syn interaction by ASC binding, samples were collected after RT-QuIC assay and ultracentrifuged to detect α-syn aggregation and co-precipitation of ASC. Immunoblotting showed that ASC is co-precipitated with α-syn after RT-QuIC assay, and the amount of insoluble α-syn was reduced in the presence of ASC (Fig. 2D, E). ASC incubated alone did not generate any Th-T signal, indicating that the recombinant protein does not possess intrinsic amyloidogenic properties. The prolongation of the lag phase was proportional to the amount of ASC added, suggesting that ASC interferes with the seeded elongation of α-syn rather than completely preventing fibril formation. To rule out the possibility that ASC binding to fibrils simply quenched Th-T fluorescence and mimicked reduced aggregation, we corroborated the kinetic data with biochemical analysis. The observed parallel decrease in sarkosyl-insoluble α-syn after the reaction confirmed that ASC genuinely reduces the amount of aggregated α-syn, rather than merely masking the dye signal.

ASC-α-syn interactions inhibit aggregation in cells

Since ASC-bound α-syn fibrils were unable to induce aggregation *in vitro*, we analyzed the effects of ASC bound α-syn in cultured cells. The human neuroblastoma cell line SH-SY5Y overexpressing α-syn were treated with α-syn fibrils premixed with ASC. ASC inhibited intracellular α-syn aggregation in a dose-dependent manner (Fig. 3A-C), suggesting that ASC binding can inhibit the recruitment of α-syn monomers to α-syn fibrils inside cultured cells as well. The extent of inhibition increased with the amount of ASC premixed with the seeds, demonstrating a dose-dependent effect. This mirrors the dose dependence observed in the cell-free RT-QuIC assay and indicates that ASC-coated fibrils retain their diminished seeding competence after being introduced into the intracellular environment.

Next, we observed the effect of ASC overexpression in α-syn aggregation. Immunostaining showed that the overexpressed ASC protein can bind to intracellular α-syn aggregates (Fig. 3D, E). Sarkosyl fractionation of cell lysates showed decreased α-syn aggregation by ASC overexpression, suggesting that the interactions between exogeneous α-syn with intracellular ASC can also inhibit α-syn aggregation (Fig. 3F, G). In agreement with the immunocytochemical colocalization of ASC with intracellular

inclusions, the sarkosyl-insoluble α-syn fraction was selectively reduced by ASC overexpression, indicating that co-expressed intracellular ASC limits the accumulation of detergent-insoluble α-syn and that the inhibitory interaction is not restricted to fibrils encountered extracellularly.

The CARD domain of ASC interacts with α-syn fibrils and inhibits aggregation

To further characterize ASC-α-syn interactions, we analyzed the interactions between α-syn and ASC domains. ASC consists of mainly two domains: the N-terminal PYD and the C-terminal CARD (Fig. 4A). We purified recombinant PYD and CARD (Fig. 4B) and analyzed its interactions with α-syn monomers and fibrils. Immunoprecipitation using anti-ASC antibodies revealed that both PYD and CARD fragments do not bind with α-syn monomers, in line with our findings regarding full-length ASC (Fig. 4C, D). However, co-precipitation assays using α-syn fibrils revealed that CARD, but not PYD, co-precipitates with α-syn fibrils (Fig. 4E-H), suggesting that ASC protein bind to α-syn fibrils using the CARD domain. ASC comprises an N-terminal PYD and a C-terminal CARD joined by a flexible linker, and both domains normally mediate homotypic interactions during inflammasome assembly. By testing the isolated domains, we localized the fibril-binding activity specifically to the CARD: the CARD

fragment reproduced the fibril co-sedimentation behavior of full-length ASC, whereas the PYD fragment remained in the supernatant, identifying the CARD as the principal α-syn fibril–binding module of ASC.

To analyze the effect of CARD binding in α-syn aggregation, we conducted an RT-QuIC assay with 1 μM of ASC, PYD, and CARD. As a result, the mixture of full-length ASC protein or CARD fragments increased the lag time for the seeded aggregation of α-syn (Fig. 5A, B). We also analyzed the effect of CARD binding in cultured cells and found that the preincubation of α-syn fibrils with ASC and CARD, but not PYD, can inhibit intracellular aggregation as well (Fig. 5C, D). Thus, the CARD fragment alone recapitulated the inhibitory activity of full-length ASC in both the cell-free and the cellular seeded-aggregation assays, whereas the PYD fragment was inert throughout, establishing a strict correspondence between fibril binding and the suppression of α-syn aggregation.

Since studies have reported that α-syn fibrils with different seeding activities and structures show different proteinase K digestion patterns, we analyzed proteinase K digestion patterns of α-syn fibrils bound to ASC, PYD, or CARD[34]. However, proteinase K digestion assay revealed that the binding of ASC and its fragments does not alter the digestion patterns of α-syn fibrils, suggesting that ASC binding does not affect the

structure of α-syn fibrils. Across the digestion time course, the proteinase K–resistant banding pattern of α-syn fibrils was indistinguishable in the presence or absence of ASC, PYD, or CARD, arguing that ASC binding neither converts the fibrils into a distinct strain-like conformation nor alters their proteolytic susceptibility. Together with the surface co-sedimentation data, this indicates that the inhibitory effect of ASC reflects occupancy of the fibril surface rather than remodeling of the fibril core.

Discussion

In our study, we have revealed that ASC monomers inhibit α-syn aggregation by direct interaction of the CARD domain and α-syn aggregates. While ASC binding increased the toxicity of amyloid β[22,23], ASC-bound α-syn aggregates failed to induce aggregation both *in vitro* and in cultured cells. This may be due to the difference in the conformation of ASC. Although amyloid β interacted with ASC specks, we observed the interaction between ASC monomers. Thus, ASC specks and monomers may have different roles in protein aggregation. The differential roles of ASC specks and monomers may also explain the negative role of increased ASC expression in synucleinopathy[14,18]. While ASC monomers can inhibit α-syn aggregation, ASC expressed in patient brains is likely to be found as inflammasomes or ASC specks. Although the interaction between ASC specks and α-syn remain unclear, our findings suggest that the formation of inflammasomes and ASC specks can interfere with the binding of ASC monomers with α-syn fibrils. A similar model has been proposed in ASC binding to caspase-1, suggesting that formation of inflammasomes and ASC specks can interfere with CARD[35]. Thus, the decreased α-syn burden by inflammasome inhibitors[17,18] may be related to increased free ASC monomers binding to α-syn aggregates.

It should be noted that overexpressed ASC can self-assemble into specks, which

raises the question of why ASC overexpression inhibited, rather than promoted, α-syn aggregation in our cells. Our immunocytochemistry showed that overexpressed ASC colocalized with intracellular α-syn aggregates (Fig. 3E), suggesting that a binding-competent pool of ASC—presumably monomeric or in a pre-speck state—remained available to engage α-syn fibrils under these conditions. Defining the oligomeric state of ASC required for α-syn binding, and whether mature specks retain or lose this inhibitory capacity, will require further study.

The selectivity of CARD in α-syn binding may be due to the difference in the electric charges of PYD and CARD. Studies have shown that α-syn fibrils expose the negatively charged C-terminal residues[36]. While both the PYD and CARD have both positively and negatively charged surfaces for self-assembly, the CARD domain possesses a positively charged surface, used to bind with other proteins in inflammasome formation[37], while the PYD uses the negatively charged surface[38]. Therefore, the negatively charged surfaces of α-syn fibrils can more easily bind to the negatively charged CARD than the PYD.

Consistent with a surface-binding mode of action, the proteinase K digestion profiles of α-syn fibrils were unchanged by ASC, PYD, or CARD, indicating that ASC binding does not remodel the fibril core. We therefore propose that monomeric ASC

inhibits aggregation by binding to the fibril surface and sterically blocking the recruitment and templated conversion of α-syn monomers, rather than by altering the conformation of pre-existing fibrils.

These observations may bear directly on the pathogenesis of PD, in which the dopaminergic neurons of the substantia nigra pars compacta are progressively lost while α-syn accumulates as Lewy pathology. The anatomically stereotyped spread of α-syn pathology is widely attributed to the prion-like, seeded conversion of endogenous α-syn—the very process that ASC suppressed in our assays. Dopaminergic neurons are thought to be especially vulnerable to this burden because their dopamine metabolism, demanding calcium handling and high basal oxidative load leave them poorly buffered against the additional stress imposed by aggregated α-syn and the inflammatory environment it provokes[39,40]. Neuroinflammation is a prominent feature of the Parkinsonian substantia nigra, and microglial NLRP3 inflammasome activation has been reported in patient tissue and in α-syn-based models, where it accelerates dopaminergic degeneration; conversely, pharmacological NLRP3 inhibition attenuates α-syn pathology and preserves dopaminergic neurons[18,41,42]. Our data offers a complementary, non-inflammatory contribution to this protection: by limiting the assembly of ASC into specks, inflammasome inhibition would spare a pool of monomeric ASC able to coat α-syn fibrils

and blunt their seeding activity. We therefore propose a balance in which monomeric ASC is neuroprotective whereas speck-associated ASC is pathogenic, a balance that may tip towards aggregation as microglial inflammasome activation increases with ageing and disease. Testing this model will require dopaminergic systems beyond the SH-SY5Y line used here—such as midbrain dopaminergic neurons, α-syn preformed-fibril rodent models and microglia–neuron co-cultures—in which the contributions of monomeric and speck ASC to dopaminergic survival can be dissected.

Overall, our study suggests the protective role of ASC monomers in α-syn aggregation. Our findings demonstrate that inhibiting inflammasome formation may not only prevent inflammation, but also may lead to preventing α-syn aggregation by ASC binding. Therefore, increasing monomeric ASC by inflammasome inhibition and other approaches may be a potential therapeutic strategy for limiting α-syn aggregation. In the specific context of PD, such a strategy would be particularly attractive because it could simultaneously dampen microglial inflammation and limit the seeded propagation of α-syn.

Acknowledgments

The authors appreciate Drs. Masato Hasegawa, Airi Tarutani (Tokyo Metropolitan Institute of Medical Science) and Michel Goedert (Medical Research Council Laboratory of Molecular Biology) for valuable reagents. The authors are also grateful to our current and previous laboratory members for helpful discussions.

Author contributions

Yukiko Hori and Taisuke Tomita supervised the study. Kohta Hirayama, Hiroto Kobayashi, and Ikumi Tomizawa carried out the biological experiments, All authors analyzed the data, discussed the results, wrote the paper and approved the final manuscript.

Funding

This work was supported in part by a Grant-in-Aid for Scientific Research (C) (JP18K06653 to Y.H), a Grant-in-Aid for Scientific Research (B) (JP21H02622, 24KJ0765 to Y.H.), a Grant-in-Aid for Scientific Research (A) (JP19H01015, JP23H00394 to T.T.), Grant-in-Aid for Transformative Research Areas (B) (JP22H05036 to Y.H.) from the Japan Society for the Promotion of Science (JSPS), Research and Development Grants for Dementia (21dk0207046 and 24dk0207061 to T.T.) from the

Japan Agency for Medical Research and Development (AMED). I.T. is a research fellow of JSPS (24KJ0765).

Competing interests

The authors declare no competing financial interests associated with this study.

Declaration of generative AI and AI-assisted technologies in the manuscript preparation process

During the preparation of this work, the author(s) used Claude for English proofreading of the manuscript. The author(s) reviewed and edited the output as needed and take full responsibility for the content of the published article.

References

1. Spillantini, M. G. *et al.* α-Synuclein in Lewy bodies. *Nature* **388**, 839–840 (1997).

2. Wakabayashi, K., Matsumoto, K., Takayama, K., Yoshimoto, M. & Takahashi, H. NACP, a presynaptic protein, immunoreactivity in Lewy bodies in Parkinson's disease. *Neurosci. Lett.* **239**, 45–48 (1997).

3. Takeda, A. *et al.* Abnormal accumulation of NACP/alpha-synuclein in neurodegenerative disorders. *Am. J. Pathol.* **152**, 367–372 (1998).

4. Tu, P. *et al.* Glial cytoplasmic inclusions in white matter oligodendrocytes of multiple system atrophy brains contain insoluble α-synuclein. *Ann. Neurol.* **44**, 415–422 (1998).

5. Baba, M. *et al.* Aggregation of alpha-synuclein in Lewy bodies of sporadic Parkinson's disease and dementia with Lewy bodies. *Am. J. Pathol.* **152**, 879–884 (1998).

6. Goedert, M., Jakes, R. & Spillantini, M. G. The Synucleinopathies: Twenty Years On. *J. Park. Dis.* **7**, S51–S69 (2017).

7. Peng, C. *et al.* Cellular milieu imparts distinct pathological α-synuclein strains in α-synucleinopathies. *Nature* **557**, 558–563 (2018).

8. Miake, H., Mizusawa, H., Iwatsubo, T. & Hasegawa, M. Biochemical characterization of the core structure of alpha-synuclein filaments. *J. Biol. Chem.* **277**, 19213–19219 (2002).

9. Fujiwara, H. *et al.* α-Synuclein is phosphorylated in synucleinopathy lesions. *Nat. Cell Biol.* **4**, 160–164 (2002).

10. Conway, K. A., Harper, J. D. & Lansbury, P. T. Accelerated in vitro fibril formation by a mutant α-synuclein linked to early-onset Parkinson disease. *Nat. Med.* **4**, 1318–1320 (1998).

11. Luk, K. C. *et al.* Exogenous α-synuclein fibrils seed the formation of Lewy body-like intracellular inclusions in cultured cells. *Proc. Natl. Acad. Sci.* **106**, 20051–20056 (2009).

12. Masuda-Suzukake, M. *et al.* Pathological alpha-synuclein propagates through neural networks. *Acta Neuropathol. Commun.* **2**, 88 (2014).

13. Karpowicz, R. J., Trojanowski, J. Q. & Lee, V. M.-Y. Transmission of α-synuclein seeds in neurodegenerative disease: recent developments. *Lab. Invest.* **99**, 971–981 (2019).

14. Fan, Z. *et al.* Systemic activation of NLRP3 inflammasome and plasma α-synuclein levels are correlated with motor severity and progression in

Parkinson's disease. *J. Neuroinflammation* **17**, 11 (2020).

15. Kelley, N., Jeltema, D., Duan, Y. & He, Y. The NLRP3 Inflammasome: An Overview of Mechanisms of Activation and Regulation. *Int. J. Mol. Sci.* **20**, 3328 (2019).

16. Cullen, S. P., Kearney, C. J., Clancy, D. M. & Martin, S. J. Diverse Activators of the NLRP3 Inflammasome Promote IL-1β Secretion by Triggering Necrosis. *Cell Rep.* **11**, 1535–1548 (2015).

17. Ou, Z. *et al.* NLRP3 Inflammasome Inhibition Prevents α-Synuclein Pathology by Relieving Autophagy Dysfunction in Chronic MPTP-Treated NLRP3 Knockout Mice. *Mol. Neurobiol.* **58**, 1303–1311 (2021).

18. Gordon, R. *et al.* Inflammasome inhibition prevents α-synuclein pathology and dopaminergic neurodegeneration in mice. *Sci. Transl. Med.* **10**, eaah4066 (2018).

19. Luque, M. *et al.* Clinically advanced NLRP3 inhibitor modulates microglial transcriptome and alleviates α-synuclein-induced progression of parkinsonism. *J. Neuroinflammation* **23**, 76 (2026).

20. Sahillioglu, A. C., Sumbul, F., Ozoren, N. & Haliloglu, T. Structural and Dynamics Aspects of ASC Speck Assembly. *Structure* **22**, 1722–1734 (2014).

21. Hoss, F., Rodriguez-Alcazar, J. F. & Latz, E. Assembly and regulation of ASC specks. *Cell. Mol. Life Sci. CMLS* **74**, 1211–1229 (2017).

22. Venegas, C. *et al.* Microglia-derived ASC specks cross-seed amyloid-β in Alzheimer's disease. *Nature* **552**, 355–361 (2017).

23. Friker, L. L. *et al.* β-Amyloid Clustering around ASC Fibrils Boosts Its Toxicity in Microglia. *Cell Rep.* **30**, 3743-3754.e6 (2020).

24. Masuda, M. *et al.* Cysteine misincorporation in bacterially expressed human alpha-synuclein. *FEBS Lett.* **580**, 1775–1779 (2006).

25. Nonaka, T., Iwatsubo, T. & Hasegawa, M. Ubiquitination of α-Synuclein. *Biochemistry* **44**, 361–368 (2005).

26. Tarutani, A. *et al.* The Effect of Fragmented Pathogenic α-Synuclein Seeds on Prion-like Propagation*. *J. Biol. Chem.* **291**, 18675–18688 (2016).

27. Nakamura, R. *et al.* Photo-oxygenation of histidine residue inhibits α-synuclein aggregation. *FASEB J.* **37**, e23311 (2023).

28. Iwai, A. *et al.* Attenuation of α-synuclein aggregation by catalytic photo-oxygenation. *Chem. Commun.* **59**, 5745–5748 (2023).

29. Chiu, Y. W. *et al.* Identification of calcium and integrin-binding protein 1 as a novel regulator of production of amyloid β peptide using CRISPR/Cas9-based

screening system. *FASEB J.* **34**, 7661–7674 (2020).

30. Tarutani, A., Arai, T., Murayama, S., Hisanaga, S. & Hasegawa, M. Potent prion-like behaviors of pathogenic α-synuclein and evaluation of inactivation methods. *Acta Neuropathol. Commun.* **6**, 29 (2018).
31. Suzuki, T. *et al.* Photo-oxygenation inhibits tau amyloid formation. *Chem. Commun.* **55**, 6165–6168 (2019).
32. Ozawa, S. *et al.* Photo-oxygenation by a biocompatible catalyst reduces amyloid-β levels in Alzheimer's disease mice. *Brain* **144**, 1884–1897 (2021).
33. Tomita, T. *et al.* The presenilin 2 mutation (N141I) linked to familial Alzheimer disease (Volga German families) increases the secretion of amyloid β protein ending at the 42nd (or 43rd) residue. *Proc. Natl. Acad. Sci.* **94**, 2025–2030 (1997).
34. Shahnawaz, M. *et al.* Discriminating α-synuclein strains in Parkinson's disease and multiple system atrophy. *Nature* **578**, 273–277 (2020).
35. Yu, T.-G. *et al.* Oligomeric states of ASC specks regulate inflammatory responses by inflammasome in the extracellular space. *Cell Death Discov.* **9**, 142 (2023).
36. Li, B. *et al.* Cryo-EM of full-length α-synuclein reveals fibril polymorphs with

a common structural kernel. *Nat. Commun.* **9**, 3609 (2018).

37. Robert Hollingsworth, L. *et al.* Mechanism of filament formation in UPA-promoted CARD8 and NLRP1 inflammasomes. *Nat. Commun.* **12**, 189 (2021).
38. Bae, J. Y. & Park, H. H. Crystal Structure of NALP3 Protein Pyrin Domain (PYD) and Its Implications in Inflammasome Assembly. *J. Biol. Chem.* **286**, 39528–39536 (2011).
39. Sohrabi, T. *et al.* Common Mechanisms Underlying α-Synuclein-Induced Mitochondrial Dysfunction in Parkinson's Disease. *J. Mol. Biol.* **435**, 167992 (2023).
40. Estefanía, S. -R. *et al.* Nigrostriatal dopaminergic vulnerability in Parkinson's disease: Neuroprotective strategies. *Neural. Regen. Res.* **21**, 3378–3386 (2026).
41. Lee, E. *et al.* MPTP-driven NLRP3 inflammasome activation in microglia plays a central role in dopaminergic neurodegeneration. *Cell Death Diff.* **26**, 213–228 (2019).
42. Wang, A. *et al.* Inhibition of NLRP3 inflammasome ameliorates LPS-induced neuroinflammatory injury in mice via PINK1/Parkin pathway. *Neuropharmacology* **257**, 110063 (2024).

Figures

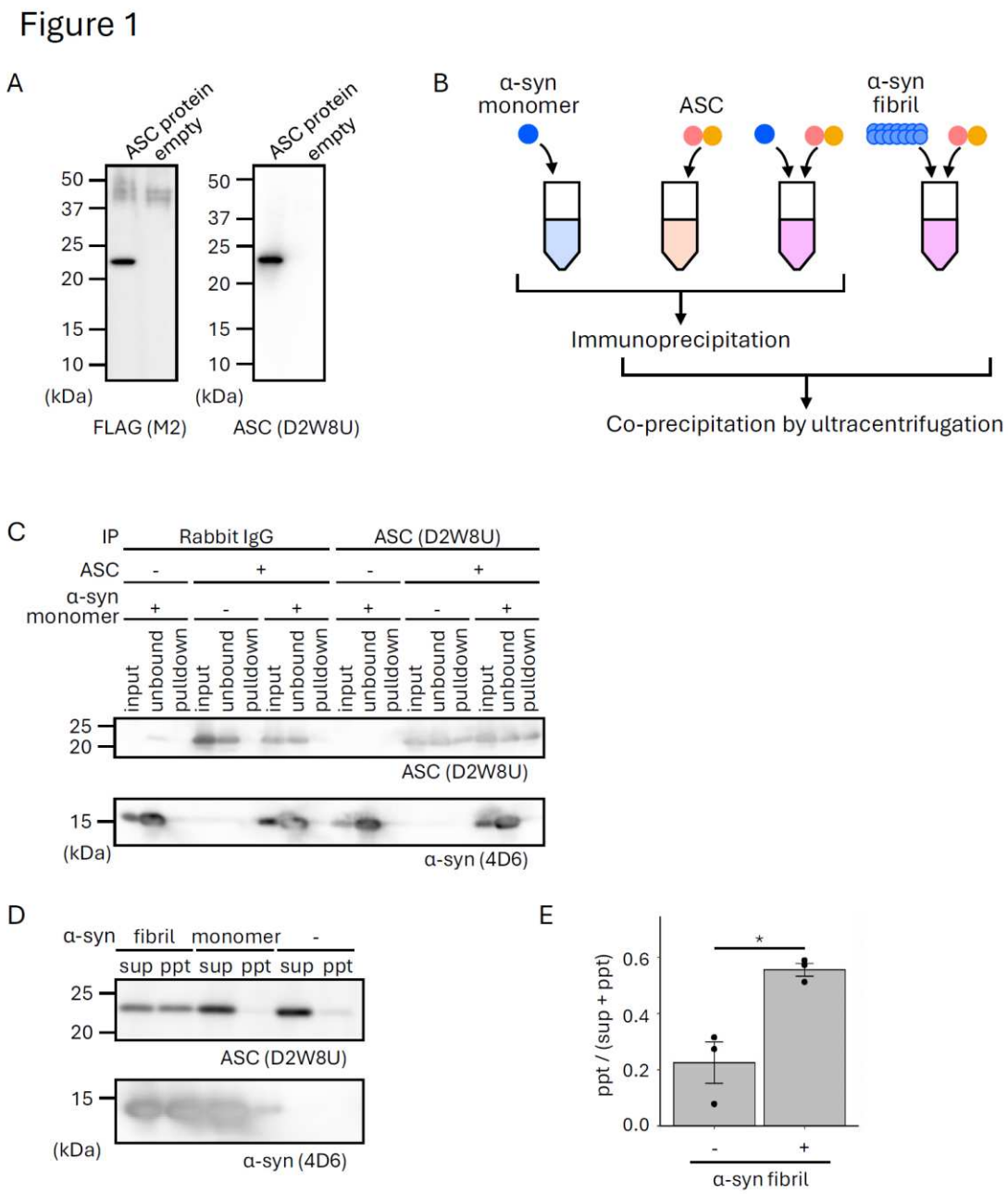

Figure 1
A
ASC protein
empty
ASC protein
empty
50
37
25
20
15
10
(kDa)
(kDa)
FLAG (M2)
ASC (D2W8U)
B
α-syn
monomer
ASC
α-syn
fibril
Immunoprecipitation
Co-precipitation by ultracentrifugation
C
IP
Rabbit IgG
ASC (D2W8U)
ASC
α-syn
monomer
input
unbound
pulldown
25
20
ASC (D2W8U)
15
(kDa)
α-syn (4D6)
D
α-syn
fibril
monomer
-
sup ppt sup ppt sup ppt
25
20
ASC (D2W8U)
15
(kDa)
α-syn (4D6)
E
ppt / (sup + ppt)
0.6
0.4
0.2
0.0
*
-
+
α-syn fibril

Fig. 1 ASC binds to α-syn fibrils.

(A) Purification of FLAG-tagged ASC was confirmed by anti-FLAG and anti-ASC antibodies.

(B) Scheme of experiments confirming the interaction of ASC and α-syn monomers or fibrils.

(C) Immunoblotting of immunoprecipitated ASC mixed with or without α-syn monomers using an anti-ASC antibody. Samples before immunoprecipitation (input), unbound proteins (unbound), and antibody-bound proteins (pulldown) were immunoblotted with anti-ASC and anti-α-syn antibodies.

(D) Immunoblotting of supernatant (sup) and precipitation (ppt) after ultracentrifugation of ASC proteins mixed with or without α-syn monomer or fibrils. Samples were immunoblotted with anti-ASC and anti-α-syn antibodies.

(E) Quantitative analysis of precipitated ASC normalized by total ASC in (D). n=3, mean ± SEM, Student t-test, *$p<0.05$

Figure 2

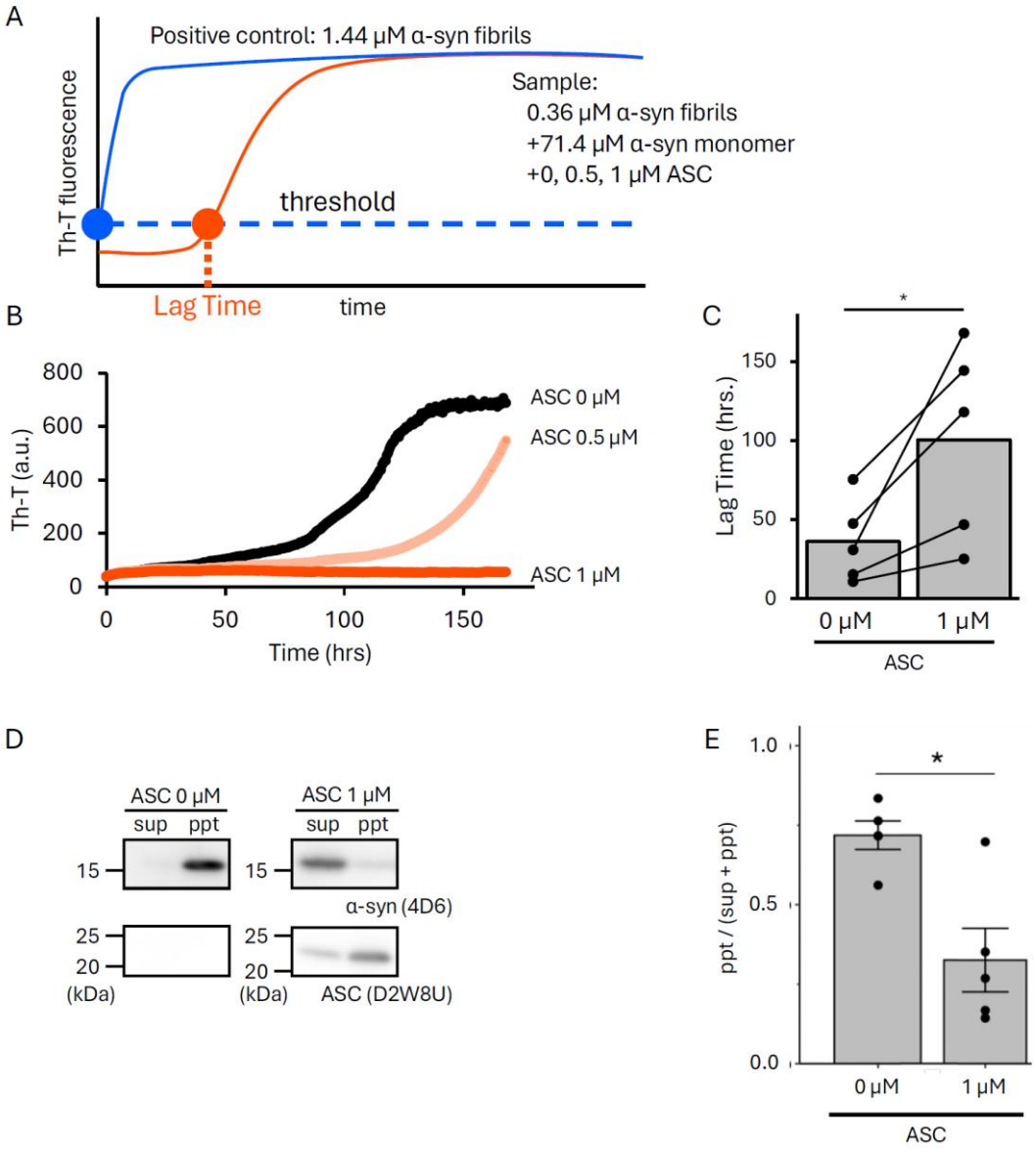


Fig. 2 ASC binding inhibits α-syn aggregation.

(A) Scheme for calculating the "lag time" from the Th-T fluorescence of α-syn from the RT-QuIC assay. Lag time was calculated as the time surpassing the threshold value;

the Th-T fluorescence of 0.4 mg/mL α-syn fibrils.

(B) Th-T fluorescence of RT-QuIC assay with 0, 0.5, 1 μM ASC monomers.

(C) Quantitative analysis of the lag time of α-syn incubated with or without ASC. n=5, mean ± SEM, paired-sample t-test, *p<0.05.

(D) Immunoblotting of samples collected and ultracentrifuged after 168 hours of RT-QuIC assay. Supernatant (sup) and precipitation (ppt) were immunoblotted with anti-ASC and anti-α-syn antibodies

(E) Quantitative analysis of precipitated α-syn normalized by total α-syn in (D). n=5, mean ± SEM, Student t-test, *p<0.05.

Figure 3

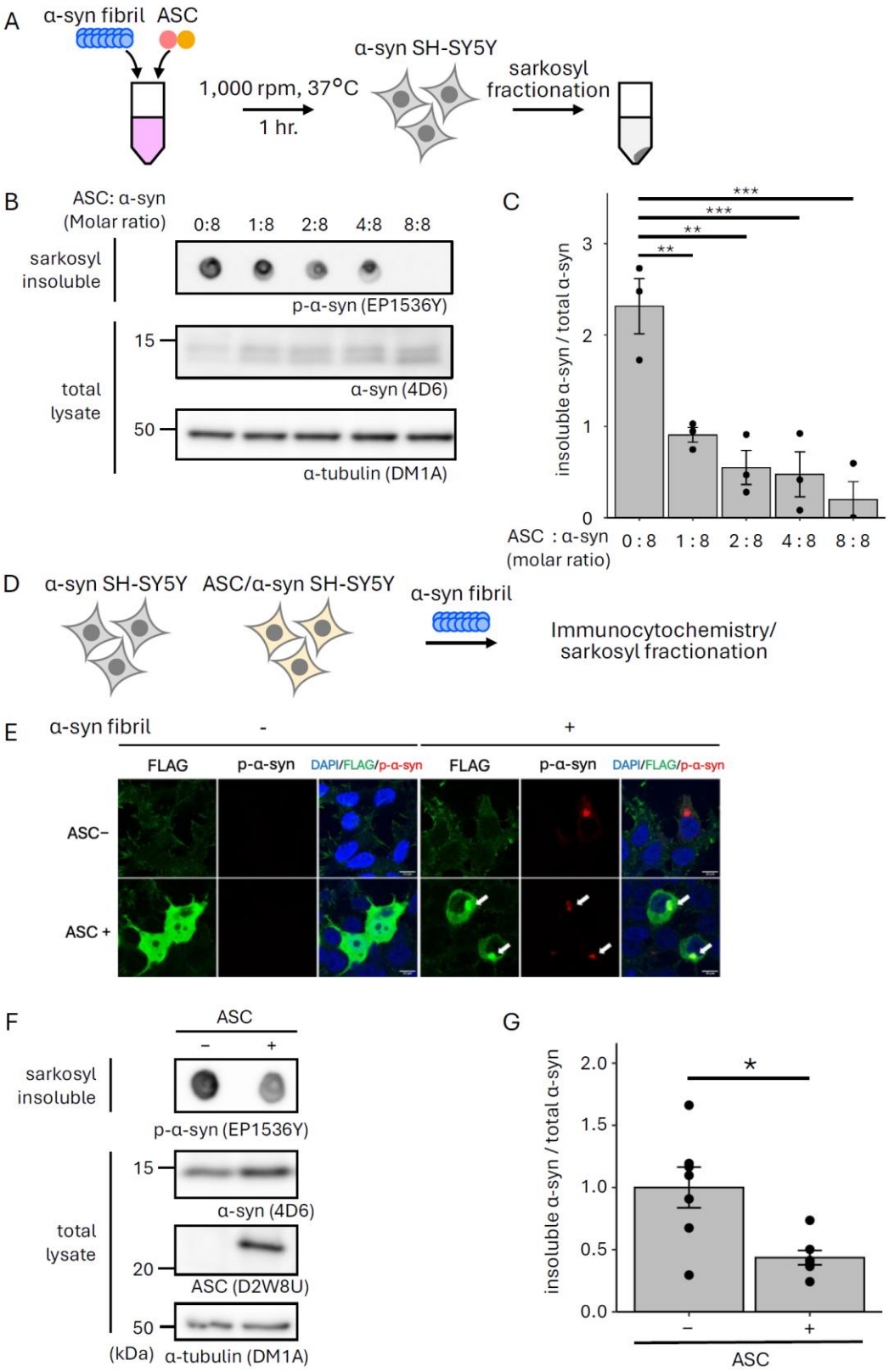

A
α-syn fibril
ASC
1,000 rpm, 37°C
1 hr.
α-syn SH-SY5Y
sarkosyl fractionation
B
ASC: α-syn (Molar ratio)
0:8
1:8
2:8
4:8
8:8
sarkosyl insoluble
p-α-syn (EP1536Y)
total lysate
15
α-syn (4D6)
50
α-tubulin (DM1A)
C
***
***
**
**
insoluble α-syn / total α-syn
0
1
2
3
ASC : α-syn (molar ratio)
0 : 8
1 : 8
2 : 8
4 : 8
8 : 8
D
α-syn SH-SY5Y
ASC/α-syn SH-SY5Y
α-syn fibril
Immunocytochemistry/ sarkosyl fractionation
E
α-syn fibril
-
+
FLAG
p-α-syn
DAPI/FLAG/p-α-syn
FLAG
p-α-syn
DAPI/FLAG/p-α-syn
ASC−
ASC +
F
ASC
−
+
sarkosyl insoluble
p-α-syn (EP1536Y)
total lysate
15
α-syn (4D6)
20
ASC (D2W8U)
50
(kDa)
α-tubulin (DM1A)
G
*
insoluble α-syn / total α-syn
0.0
0.5
1.0
1.5
2.0
−
+
ASC

Fig. 3 ASC inhibits the seeding activity of α-syn fibrils

(A) Scheme of inducing intracellular aggregation using α-syn fibrils with or without ASC in SH-SY5Y cells overexpressing α-syn (α-syn SH-SY5Y).

(B) Immunoblotting of the sarkosyl insoluble fraction and total lysates of α-syn SH-SY5Y induced by α-syn fibrils incubated with ASC at the indicated molecular ratios.

(C) Quantitative analysis of insoluble α-syn normalized by total α-syn in (B). n=3, mean ± SEM, Tukey-HSD test, **p<0.01, ***p<0.0005.

(D) Scheme of seeded aggregation induced in α-syn SH-SY5Y and α-syn SH-SY5Y overexpressing ASC (α-syn/ASC-SHSY5Y).

(E) Immunocytochemistry of phosphorylated α-syn (p-α-syn) and FLAG-tagged ASC.

(F) Immunoblotting of the sarkosyl insoluble fraction and total lysates of α-syn SH-SY5Y and ASC/α-syn SH-SY5Y cells induced by α-syn fibrils.

(G) Quantitative analysis of insoluble α-syn normalized by total α-syn in (B). n=6, mean ± SEM, Student t-test, *p<0.05.

Figure 4

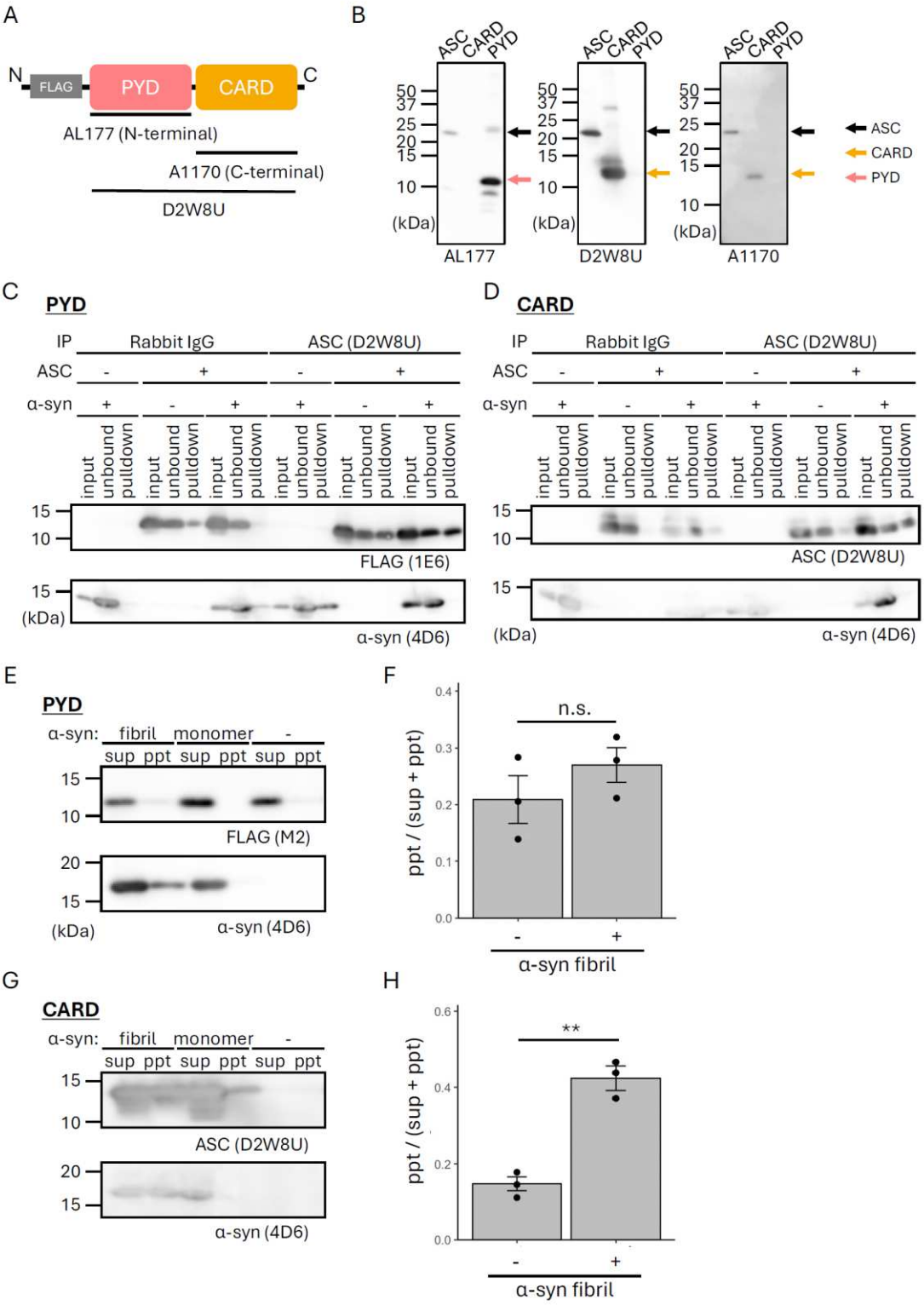

A
N
FLAG
PYD
CARD
C
AL177 (N-terminal)
A1170 (C-terminal)
D2W8U
B
ASC
CARD
PYD
50
37
25
20
15
10
(kDa)
AL177
D2W8U
A1170
C
PYD
IP
Rabbit IgG
ASC (D2W8U)
ASC
α-syn
input
unbound
pulldown
FLAG (1E6)
α-syn (4D6)
D
CARD
ASC (D2W8U)
E
PYD
α-syn:
fibril
monomer
sup
ppt
FLAG (M2)
F
n.s.
ppt / (sup + ppt)
α-syn fibril
G
CARD
ASC (D2W8U)
H
**

Fig. 4 ASC binds to α-syn at the CARD domain

(A) Diagram of ASC domains and epitopes of anti-ASC antibodies used.

(B) Immunoblotting of purified ASC, PYD, and CARD using three different anti-ASC antibodies. The arrows indicate ASC (black), PYD (pink), and CARD (yellow) specific bands.

(C) Immunoblotting of immunoprecipitated PYD mixed with or without α-syn monomers using an anti-ASC antibody. Samples before immunoprecipitation (input), unbound proteins (unbound), and antibody-bound proteins (pulldown) were immunoblotted with anti-FLAG and anti-α-syn antibodies.

(D) Immunoblotting of immunoprecipitated CARD mixed with or without α-syn monomers using an anti-ASC antibody. Samples before immunoprecipitation (input), unbound proteins (unbound), and antibody-bound proteins (pulldown) were immunoblotted with anti-ASC and anti-α-syn antibodies.

(E) Immunoblotting of supernatant (sup) and precipitation (ppt) after ultracentrifugation of PYD proteins mixed with or without α-syn monomer or fibrils. Samples were immunoblotted with anti-FLAG and anti-α-syn antibodies.

(F) Quantitative analysis of precipitated PYD normalized by total PYD in (E). n=3, mean ± SEM, Student t-test, n.s. not significant.

(G) Immunoblotting of supernatant (sup) and precipitation (ppt) after ultracentrifugation of CARD proteins mixed with or without α-syn monomer or fibrils. Samples were immunoblotted with anti-ASC and anti-α-syn antibodies.

(H) Quantitative analysis of precipitated CARD normalized by total CARD in (D). n=3, mean ± SEM, Student t-test, **p<0.01.

Figure 5

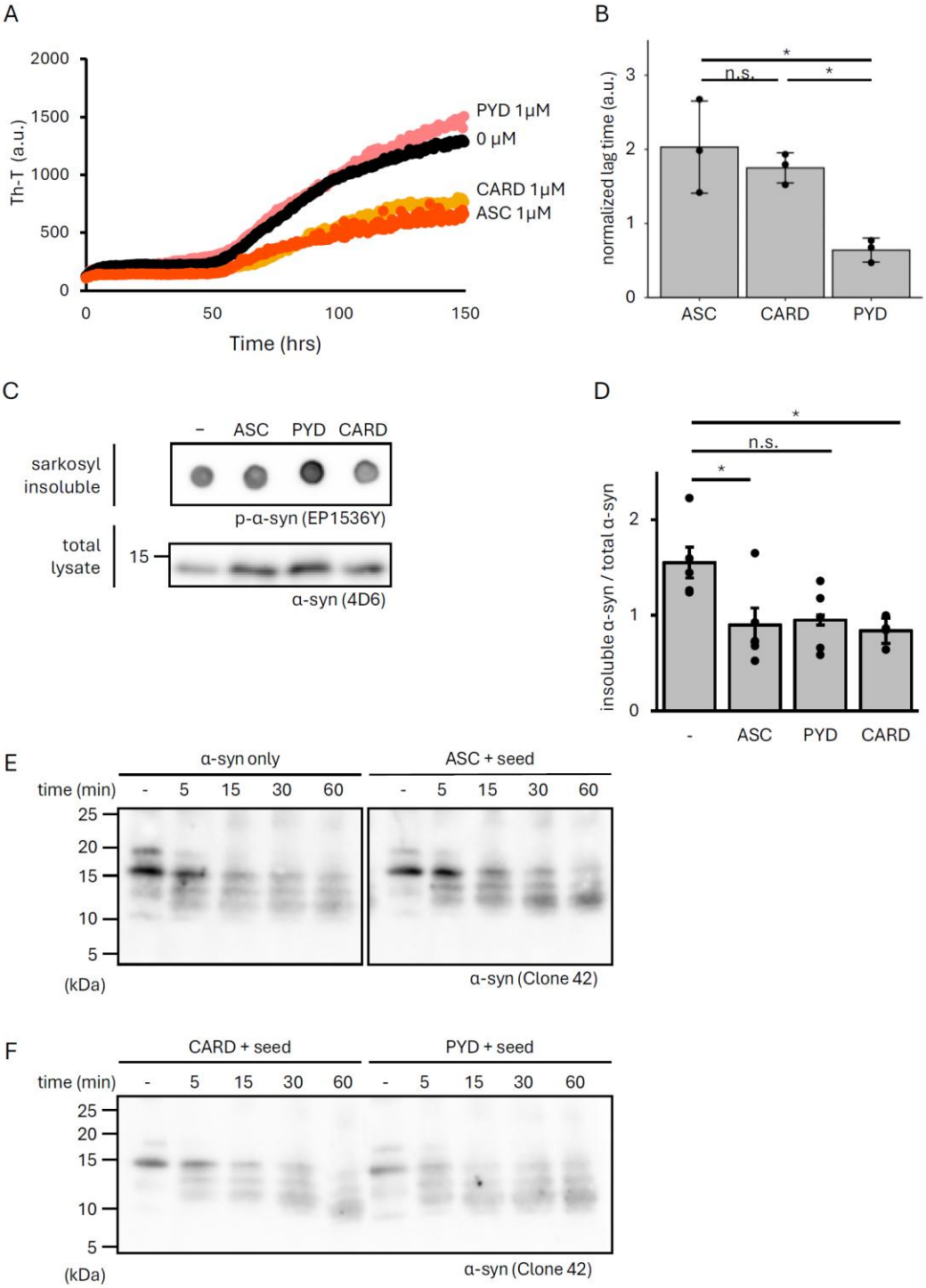

A
2000
1500
1000
500
0
Th-T (a.u.)
0
50
100
150
Time (hrs)
PYD 1μM
0 μM
CARD 1μM
ASC 1μM
B
normalized lag time (a.u.)
3
2
1
0
*
n.s.
*
ASC
CARD
PYD
C
–
ASC
PYD
CARD
sarkosyl insoluble
p-α-syn (EP1536Y)
total lysate
15
α-syn (4D6)
D
insoluble α-syn / total α-syn
2
1
0
*
n.s.
*
-
ASC
PYD
CARD
E
α-syn only
ASC + seed
time (min)
- 5 15 30 60
- 5 15 30 60
25
20
15
10
5
(kDa)
α-syn (Clone 42)
F
CARD + seed
PYD + seed
time (min)
- 5 15 30 60
- 5 15 30 60
25
20
15
10
5
(kDa)
α-syn (Clone 42)

Fig. 5 The CARD domain inhibits α-syn aggregation

(A) Th-T fluorescence of RT-QuIC assay with ASC, PYD, or CARD.

(B) Quantitative analysis of the lag time of α-syn incubated with ASC, PYD, or CARD in (A). n=3, mean ± SEM, Tukey HSD t-test, *p<0.05, n.s. not significant.

(C) Immunoblotting of the sarkosyl insoluble fraction and total lysates of α-syn SH-SY5Y cells overexpressing ASC, PYD, or CARD induced by α-syn fibrils.

(D) Quantitative analysis of insoluble α-syn normalized by total α-syn in (C). n=5, mean ± SEM, Student t-test, *p<0.05, n.s. not significant.

(E) Proteinase K analysis of α-syn fibrils with and without ASC protein. The α-syn fibrils were incubated with proteinase K for 0, 5, 15, 30, 60 minutes and band patterns were observed by immunoblotting.

(F) Proteinase K analysis of α-syn fibrils with PYD and CARD.

Supplementary Files

This is a list of supplementary files associated with this preprint. Click to download.

- ASCsupplementary.pdf